The Interactions of Gravity Waves with Mesocyclones:

Preliminary Observations and Theory

DRAFT, UNDER REVIEW

TIMOTHY A. COLEMAN AND KEVIN R. KNUPP

Department of Atmospheric Science, The University of Alabama in Huntsville

Apparent interactions between ducted gravity waves and pre-existing mesocyclones are investigated. Preliminary analyses of WSR-88D radar observations from several cases reveal that the intersection of fine lines, whose propagation speed is consistent with that of gravity waves, and existing mesocyclones leads to an increase in rotational velocity of the mesocyclone. Utilizing simplified ducted wave kinematics and the vorticity equation, changes in vorticity associated with convergence/divergence and perturbation wind shear within the gravity wave are examined. Convergence ahead of wave ridges may be significant, causing mesocyclone intensification through vorticity stretching. It will also be shown that a wave may significantly change the vertical wind shear and streamwise vorticity in storm inflow. A simple one-dimensional model is presented, which shows that vorticity decreases temporarily ahead of the wave ridge, then increases rapidly behind the ridge as positive tilting and stretching act together. The mesocyclone vorticity reaches a peak just ahead of the wave ridge, then begins to rapidly decrease behind the ridge. Model results compared very well to actual measurements in a sample case in which a mesocyclone interacted with two gravity waves of different amplitudes.

1. Introduction

Examination of Doppler radar data from several thunderstorms containing pre-existing mesocyclones has revealed an intriguing pattern, in which one or more relatively narrow bands of radar reflectivity approach the storm from its right flank (generally from a southerly direction). Then, upon interaction with the storm, there is an intensification of the mesocyclone and sometimes tornadogenesis. The reflectivity bands in these cases, however, can not be attributed to density currents or outflow boundaries from other storms, but instead appear to be ducted gravity waves.

The interactions between gravity waves and deep convection have been well-investigated. Many have discussed the initiation or enhancement of convection by gravity waves (e.g., Uccellini 1975; Stobie et al. 1983; Koch et al. 1988; Corfidi 1998; Koch et al. 1998). Conversely, several others have shown that convective storms can also initiate gravity waves (e.g., Alexander et al. 1995; Bosart and Cussen 1973). The relationship known as wave-CISK, whereby convective lines and gravity waves synergistically support one another, has been well-examined also (e.g., Cram et al. 1992; Raymond 1984). However, the interactions between gravity waves and mesocyclones and tornadoes have received limited attention, most of it observational in nature.

Miller and Sanders (1980) found that tornadogenesis increased within some convective regions when wave packets overtook those regions during the Super Outbreak of 3-4 April 1974. They posed a question in their paper as to whether or not the waves contained vorticity which aided the development of tornadoes. Uccellini (1975) also observed enhanced storm development and tornadoes in conjunction with waves in Iowa on 18 May 1971. More recently, Kilduff (1999) observed an increase in Doppler radar-observed storm

rotational velocities in a mesocyclone upon interaction with gravity waves on 22 January 1999 in northwest Alabama. Barker (2006) similarly finds a link between what he terms "reflectivity tags" moving quickly through a linear MCS and tornadogenesis, in the case of the F3 Evansville, Indiana tornado of 6 November 2005. The environment and dynamics of these tags are consistent with gravity waves.

In this paper, we examine the following hypothesis: gravity waves, upon interaction with pre-existing mesocyclones, may significantly alter the vorticity of those mesocyclones, and may in some cases produce tornadogenesis. In section 2 of this paper, the kinematics of ducted gravity waves are reviewed, and the dynamics of wave/mesocyclone interactions are examined. In section 3, the development and results of a simplified 1-D model are presented. In section 4, the 22 January 1999 case are examined in detail using Doppler radar data, with results compared to those predicted by the 1-D model. Additional cases of apparent gravity wave interaction with mesocyclones and/or tornadoes are also listed. Conclusions and future work are presented in section 5.

2. Theory

a. Kinematics of ducted gravity waves

Internal gravity waves may be initiated by convection, geostrophic adjustment, topography, and shear instability (Koch and O'Handley 1997). Waves may be reflected by layers with large vertical gradients of vertical wavelength m associated with gradients in the Scorer parameter l (Scorer 1949) through $m^2 = l^2 - k^2$, where

$$l^2 = \frac{N^2}{(U-c)^2} - \frac{\frac{\partial^2 U}{\partial z^2}}{U-c} \qquad (1)$$

and k is the horizontal wavelength, c is the ground-relative wave phase speed, U is the mean wave-normal background wind in the duct, and N is the Brunt-Vaisala frequency. These layers contain vertical gradients in static stability

and/or wind shear. Waves may also be reflected by the ground. Lindzen and Tung (1976) showed that waves may be "ducted", in situations where an upward- and a downward-moving internal wave are trapped between the surface and a reflecting layer, and the two waves constructively interfere. The depth of the duct must be ¼ of a vertical wavelength, and must contain no critical level (Lindzen and Tung 1976). They also found that the intrinsic phase speed for the n mode ducted wave is given by $c - U = ND\pi^{-1}(½ + n)^{-1}$, where $n = 0, 1, 2, …,$ and D is the depth duct. Therefore, the phase speed of ducted gravity waves in a given environment may be determined through analysis of vertical profiles of ambient temperature and wind.

Assuming linear waves, the wind perturbations within an internal gravity wave may be written as $u' = A \cos (kx-\omega t+mz)$, where k is the horizontal wavenumber and m is the vertical wavenumber (the sign of the mz term is positive for an upward-propagating wave and negative for a downward-propagating wave). Fig. 1 illustrates the perturbation airflow vectors at $t=0$ for an upward and downward moving wave (both also moving to the right) with horizontal wavelength 50 km and vertical wavelength 8 km. Now, supposing a wave-reflecting level at 2 km AGL, and assuming a perfect reflector (no change in amplitude upon reflection and no phase shift), the two waves would constructively interfere within the duct between 0 and 2 km AGL, producing the perturbation airflow vectors in Figure 2. It may be shown that the magnitude of divergence is largest near the surface, with convergence ahead of the wave ridge and divergence ahead of the wave trough. Perturbation vertical wind shear is maximized at the top of the duct, with positive perturbation shear centered in the wave trough and negative perturbation shear centered in the wave ridge (see Fig. 2).

b. Wave/vortex interaction

Although there are a myriad of effects that a gravity wave may have on a pre-existing mesocyclone, only the two most significant, both of which affect vertical vorticity, are considered here. First, the *stretching* of pre-existing vorticity due to perturbation horizontal divergence in the wave may significantly alter

the vorticity within a mesocyclone. Also, the perturbation vertical wind shear in the wave produces horizontal vorticity, the streamwise portion of which may be *tilted* into the vertical.
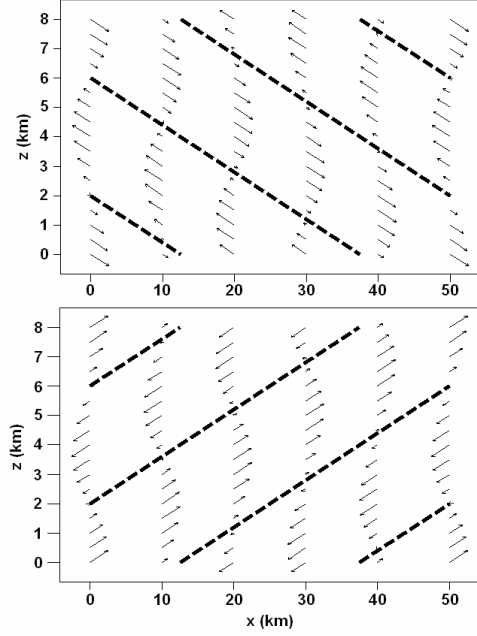

Figure 1. Airflow vectors and phase lines (heavy dashed lines) in the *x-z* plane for an upward (top) and downward (bottom) moving internal gravity wave. Distance units are in km.
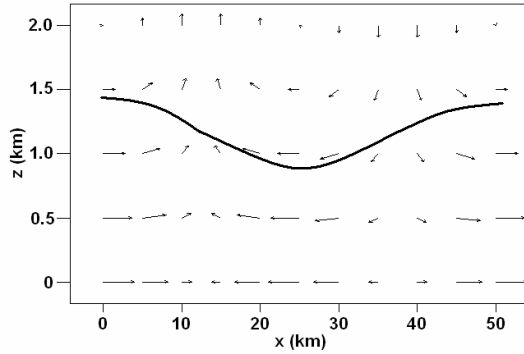

Figure 2. Airflow vectors and isentrope (heavy solid curve) in the *x-z* plane for a ducted gravity wave. Distance units are as in Fig. 1. Note the purely horizontal motion at the surface and purely vertical motion at the top of the duct ($z = 2$ km).

Considering only these two processes, the vorticity equation for the mesocyclone may be written as

$$\frac{D\zeta}{Dt} = -\zeta\frac{\partial u'}{\partial x} + \left(\frac{\partial u'}{\partial z}\frac{\partial w}{\partial n}\sin\alpha\right) \quad (2)$$

where ζ is vertical vorticity, u' is the perturbation wind in a wave (moving in the *x* direction), *n* is distance in the direction of the storm-inflow vector, and α is the angle between the wave motion vector and the storm-inflow vector. The geometry of the interaction is illustrated in Figure 3. Note that sin α is maximized when the wave is moving 90 degrees to the right of the storm inflow, such that the perturbation vertical shear vector is also at a right angle to the storm inflow. This allows the associated horizontal vorticity vector to be aligned perfectly with the storm inflow, i.e., making all the perturbation horizontal vorticity *streamwise* (e.g., Davies-Jones 1984).

We will consider a wave approaching the right flank of a storm (from the left of the inflow vector), which is the most common situation in observed case studies. Vorticity amplification through stretching, and vorticity generation through tilting, are of opposite sign in many parts of the wave. The process that dominates may be determined by several factors, such as the horizontal wavelength of the wave, the duct depth, and the angle α from which the
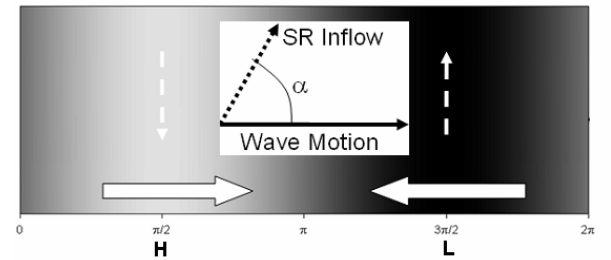

Figure 3. Geometry of wave/mesocyclone interaction in the *x-y* plane. Shading indicates wave phase. Low-level *u'* (broad white arrows), horizontal vorticity vectors associated with wave perturbation wind shear (thin dashed), wave motion (thin solid) and SR inflow vector (dotted). Note that as angle α (and therefore sin α) increase, horizontal vorticity becomes more parallel to SR inflow, ie., more streamwise.

wave approaches the storm inflow. It may be shown that, for typical mesoscale gravity waves, the vorticity increase produced by stretching is larger.

In theory, the wave trough exhibits an absence of divergence (i.e., the stretching is negligible), but it is associated with a maximum in positive perturbation shear, which through tilting contributes to an increase in ζ. Behind the trough, the tilting decreases, but convergence increases ζ through stretching. As the wave ridge approaches, stretching continues to increase vorticity, while negative perturbation shear in the ridge negates some of the stretching. Behind the ridge, divergence and negative shear would decrease vorticity, until the next wave trough approached, with positive shear offsetting some of the vorticity decrease by divergence. The time-line of these processes, relative to the gravity wave ridge/trough, is shown in Fig. 4.
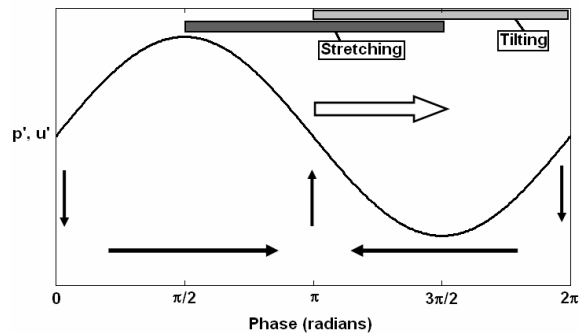

Figure 4. Regions of positive gravity wave-induced stretching (dark gray shaded box) and tilting (light gray shaded box), relative to gravity wave phase. Airflow vectors in the *x-z* plane are shown (bold arrows, not to scale), along with the phase of the ducted gravity wave (*p'* or *u'*, sine wave). Wave is moving to the right, as indicated by broad arrow.

3. Development of 1-D model

The fundamental physics of the gravity wave/mesocyclone interaction may be explained using a fairly simple model. A one-dimensional model was developed to simulate this interaction. This model assumes that the pre-existing mesocyclone is a solid-body rotator with some initial vorticity, co-located with the storm updraft. The model introduces a ducted

gravity wave, simulated by a sinusoidal disturbance in *u'*, and analyzes the change in vorticity in the mesocyclone as the entire wavelength interacts with it.

The amplitude of the wind perturbations in the wave (in m s^{-1}), its horizontal wavelength, the depth of the wave duct, and the wave motion vector are input parameters that describe the ducted gravity wave. The storm motion vector is also input, since the storm-relative motion of the wave significantly affects the vorticity change. The storm inflow vector must be input as well, so that sin α (streamwise portion of wave-associated horizontal vorticity, see section 2b) may be determined. Finally, an estimate of d*w*/d*n* (horizontal gradient in vertical motion of the storm updraft along the storm-inflow vector) must be input. A value of 2×10^{-3} s^{-1} is assumed herein, based on a low-level updraft of 10 m/s and an updraft *radius* of 5 km, which is consistent with numerical simulations of supercell storms (e.g., Droegemeier et al. 1993).

a. Example simulation

The output from an example simulation, assuming an initially weak mesocyclone interacting with a typical mesoscale gravity wave, is shown in Figure 5. The following values were input: mesocyclone initial vorticity 3×10^{-3} s^{-1}; wave amplitude 5 m s^{-1}; horizontal wavelength 50 km; duct depth 2.5 km; wave motion from 180 degrees at 25 m s^{-1}; storm motion from 250 degrees at 25 m s^{-1}; and storm-relative inflow from 140 degrees at 25 m s^{-1}.

In this simulation, the mesocyclone interacts with the wave trough first. Early on (through about 1/10 of a wave period), the negative effect on the vorticity tendency of divergence ahead of the wave trough dominates the positive effect of tilting of positive perturbation shear, decreasing ζ slightly (to 2.8×10^{-3} s^{-1}). But, after that time, the positive effect of tilting dominates, allowing ζ to increase with time. In the region behind the wave trough, rapid vorticity increase occurs, as convergence produces positive stretching in the presence of a positive contribution from tilting. As the wave ridge approaches, convergence continues to dominate despite the negative effect of tilting, with the vorticity tendency remaining positive (as large as 4.4×10^{-6} s^{-2}) until a time just before

the wave ridge, when vorticity reaches its maximum value (9.3×10^{-3} s^{-1}). Behind the ridge, negative tilting continues, in addition to divergence, so the vorticity decreases rapidly.

The interaction between the gravity wave and the mesocyclone updraft clearly has a significant effect on the mesocyclone vertical vorticity. After a brief decrease, ζ increases to *three times* its initial value at a point just ahead of the wave ridge. The vorticity then decreases rapidly behind the wave ridge. Interestingly, in this one-dimensional simulation, the net result of the interaction with one wavelength of a gravity wave is an increase in mesocyclone vorticity. This is a fascinating and unexpected result. In

the simulation, if the wave approaches the storm inflow from its left, there is a net decrease in vorticity.

b. Factors affecting mesocyclone intensification

Numerous simulations, similar to the one described in the preceding section, were performed. The initial mesocyclone vorticity in all simulations was 3×10^{-3} s^{-1}. The effect on the maximum instantaneous vorticity due to varying wave amplitude, wavelength, duct depth, wave speed, and the angle between the inflow vector and the wave motion vector are
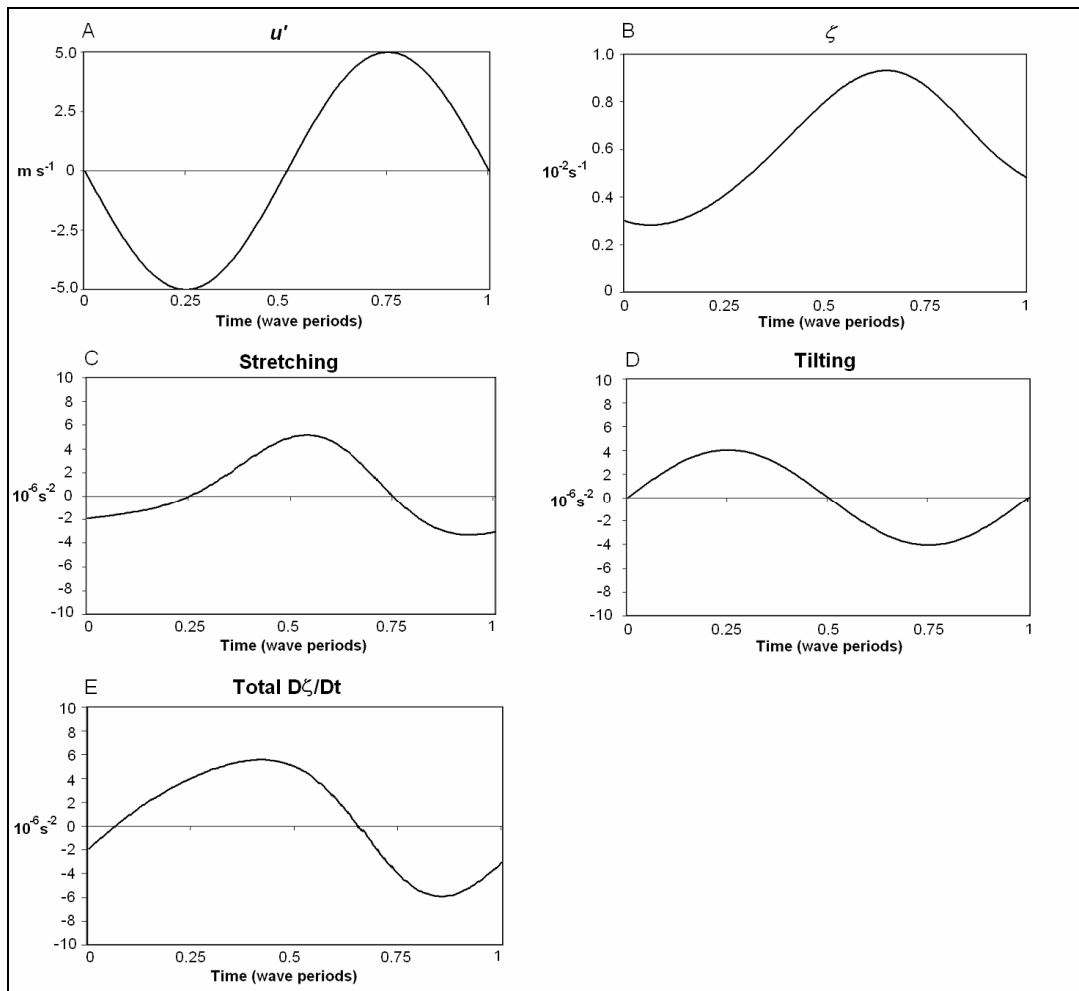

Figure 5. 1-D numerical simulation of a mesocyclone interacting with one full wave period of a gravity wave. a) u' (m s^{-1}), b) mesocyclone vorticity (10^{-2} s^{-1}), c) stretching term (10^{-6} s^{-2}), d) tilting term (10^{-6} s^{-2}), and e) total $D\zeta/Dt$ (10^{-6} s^{-2}).
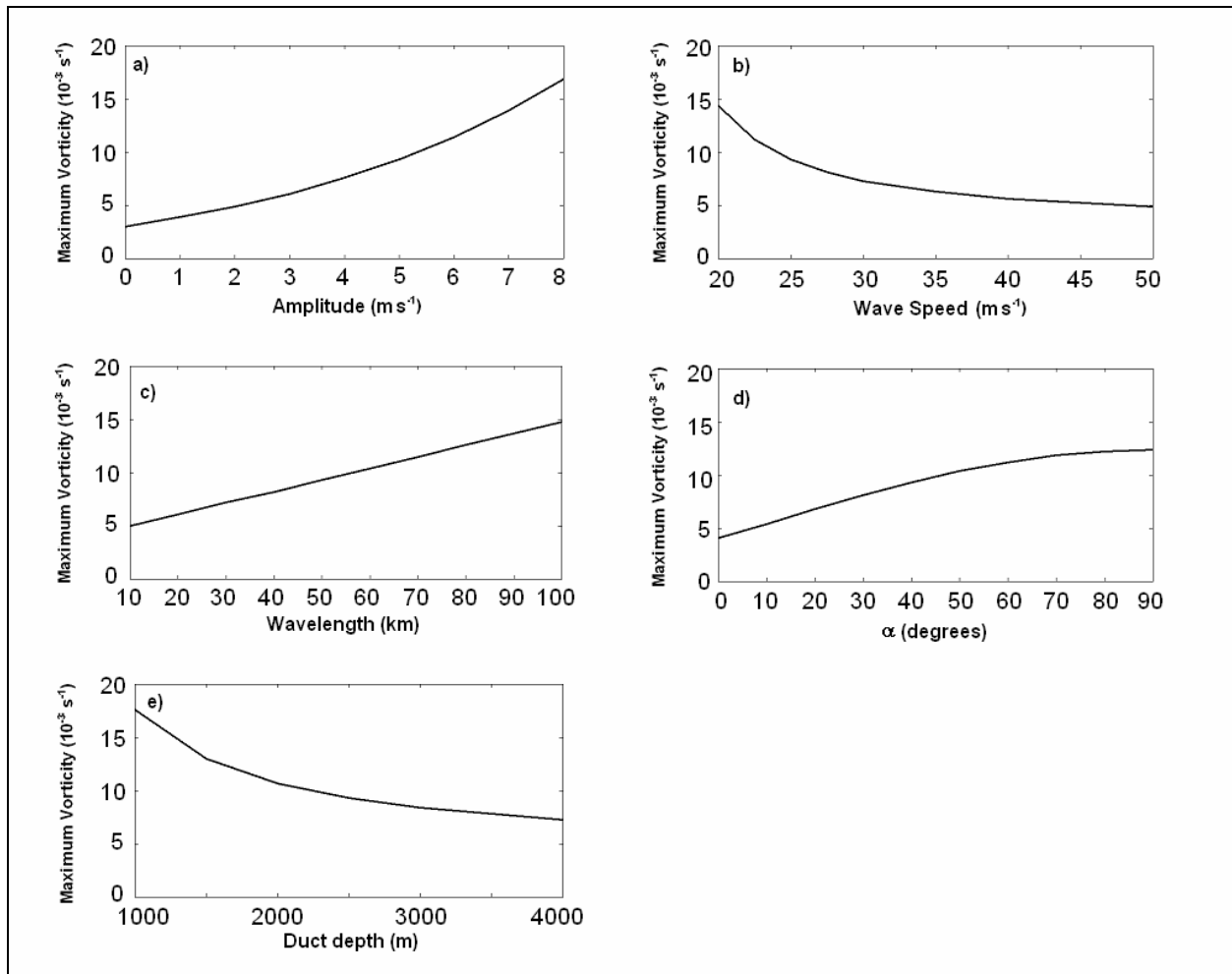
Figure 6. The effect of varying a) amplitude (m s^{-1}), b) wave speed (m s^{-1}), c) wavelength (km), d) α, the angle between the wave motion vector and the storm inflow vector (degrees), and e) the duct depth (m) on the maximum vorticity (10^{-3} s^{-1}) attained by mesocyclone in simulations described in section 3b.

summarized in Figure 6. In each simulation, all parameters were set to the same values used in the simulation described in section 3a, except for the parameter in each case whose effect was being evaluated.

Figure 6 indicates that the maximum mesocyclone vorticity produced by the interaction with a gravity wave (i) increases exponentially as the amplitude of the wave increases, (ii) increases roughly linearly as wavelength increases, and (iii) increases logarithmically as the angle α increases. Maximum vorticity decreases as wave speed and duct depth increase.

4. Case studies

It is important to emphasize that the potential interaction of gravity waves with mesocyclones was not discovered theoretically; it was actually discovered in radar observations. At the time of this writing, 16 cases have been identified that display this potential interaction. Three are presented in this introductory paper. Typically, analysis of a case involves analysis of proximity sounding data, including a vertical profile of m^2, to determine the potential of the environment to maintain ducted gravity waves and to determine their theoretical speed. Radar

data are analyzed in depth, including vertical cross-sections. Surface data are examined where available.

One case, the 22 January 1999 wave/mesocyclone interaction, will be examined in depth herein, including a comparison with a simulation from the model described in Section 3. Two others, the F4 tornado in Tuscaloosa, Alabama on 16 December 2000, and the F5 tornado near Birmingham, Alabama on 8 April 1998, are presented is less detail to demonstrate that similar patterns occur for other cases. Detailed analyses of additional cases will be deferred to later papers.

a. 22 January 1999, Northwest Alabama

On 22 January 1999, two radar fine lines, which will be shown to represent the ridges of ducted gravity waves, interacted with a pre-existing mesocyclone, intensifying it in a periodic pattern.

1) ENVIRONMENT

A marginally unstable (surface-based CAPE ~100 J kg^{-1}) but very high-shear environment existed over Alabama. The 1800 UTC sounding data from Birmingham (BMX) (Fig. 7) indicates a deep stable layer between approximately 500 and 2000 m AGL, above a 500 m-deep surface-based mixed layer. Static stability decreases above 2000 m AGL. The vertical wind shear is also rather significant, with winds veering with height (about 50 degrees over the lowest 2 km AGL) and speeds increasing from 14 to 25 m s^{-1} over that same layer. The 0-2 km AGL bulk shear is 18.3 m s^{-1}.
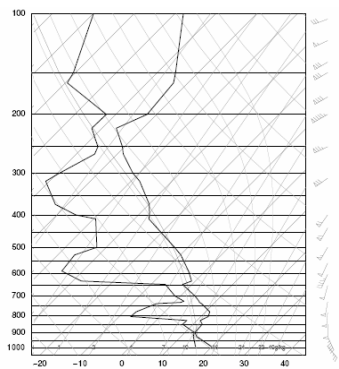

Figure 7. Skew T-ln p diagram and winds for sounding at BMX (Birmingham, AL) at 1800 UTC on 22 January 1999
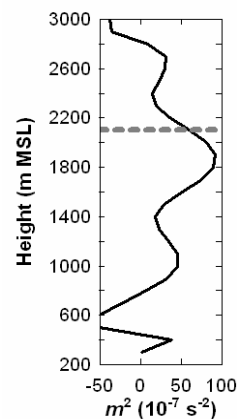

Figure 8. Vertical profile of m^2 (10^{-7} s^{-2}) using sounding data and observed wavelength and wave direction of motion (see text)

A vertical profile of m^2 was constructed (Fig. 8) using sounding wind and thermodynamic data and subsequent values of the Scorer parameter (see section 2a), and assuming a horizontal wavelength of 40 km and wave motion direction of 180 degrees for calculation of U in Eq. 1. Since this clearly shows a sharp gradient in m^2 around 2100 m MSL (Fig. 8), we assume that this defines the top of the duct. Analysis of this sounding data according to the ducting parameters of Lindzen and Tung (1976), using a duct depth of 1900 m, and $N = 0.0126$ s^{-1} indicates that this environment would support ducted gravity waves with phase speed $c = 37.8$ m s^{-1}. The synoptic-scale pattern (e.g., Koch and O'Handley 1997; Uccellini and Koch 1987) with a deep upper trough in the central part of the U.S., and a jet maximum apparently having rounded the base of the 300 hPa trough during the day on 22 January 1999, provided a background favorable for wave generation. In addition, the large wind shear could have also contributed to wave generation (e.g., Lalas and Einaudi 1976).

2) INTERACTION

Rapidly developing severe convection moved into extreme western Alabama around 2000 UTC. Around the same time, a pair of mesoscale gravity waves appeared on radar as two fine lines of enhanced reflectivity. These fine lines likely indicate the locations of the

crests of gravity waves, since the environment (synoptic and local) is favorable for gravity wave genesis and propagation, and since these bands moved so rapidly northward at 34 m s^{-1}, which is close to the predicted ducted wave speed, 37.8 m s^{-1}. It should be noted that the air mass later in the day and farther west, closer to the incoming convection, could have been slightly more unstable, causing the slightly lower phase speeds.

Radar reflectivity data from the KBMX (Birmingham, AL) WSR-88D show a mature, intense convective storm in progress at 2026 UTC (Fig. 9). This storm appears to be part of a broken quasi-linear convective system (QLCS), which had been in existence at least since 1934 UTC. Based on storm-relative velocity data at 2026, the storm contained a broad mesocyclone, with vorticity around 0.6 x 10^{-2} s^{-1}. Two apparent wave ridges are also indicated in the reflectivity panels at 2026 to the ESE and SE of the storm. At 2047 UTC, just after the initial wave ridge appears to have intersected the mesocyclone, the mesocyclone is more well-defined, and its vorticity had increased from 0.5 x 10^{-2} s^{-1} to 1.2 x 10^{-2} s^{-1} in only about 15 minutes. By 2102 UTC, the second wave ridge is interacting with the mesocyclone, and the vorticity has further increased to almost 2 x 10^{-2} s^{-1}. The radar presentation of the mesocyclone is impressive at 2102 UTC, with what may be a bounded weak echo region (BWER) in the reflectivity image and gate-to-gate, maximum rotational velocity in the storm-relative velocity image. Shortly after 2102 UTC, a small tornado touched down in northern Fayette County (Kilduff 2006, personal communication).

3) NUMERICAL SIMULATION

The 22 January 1999 wave/mesocyclone interaction event was numerically simulated using the one-dimensional model discussed in section 3. Multiple volume scans of Doppler velocity data were used to calculate *u'* within the wave ridges of both gravity waves (4.1 and 10.7 m s^{-1}). These values, along with the initial vorticity (0.5 x 10^{-2} s^{-1}), storm motion (from 240 degrees, 20 m s^{-1}), wave motion (from 180 degrees, 32 m s^{-1}), storm inflow (from 130 degrees at 25 m s^{-1}), wavelength (40 km), and duct depth (1900 m) were input into the model.

The simulated mesocyclone vorticity changes associated with the interaction with both gravity waves were quite similar to the observed vorticity changes. Figure 10 shows a comparison of observed vs. simulated vorticity over the 2 wave periods. The model time was synchronized with observations by assuming that the interaction began in the trough ahead of the first wave ridge visible on radar. Note that the simulation slightly underestimates the vorticity increase associated with the first gravity wave (0.84 x 10^{-2} s^{-1} simulated vs. 1.2 x 10^{-2} s^{-1} observed), and also shows the first vorticity maximum occurring a few minutes too early. However, the timing and magnitude of the significant vorticity increase associated with the second wave ridge is simulated very well. Peak vorticity values are close (2.3 x 10^{-2} s^{-1} simulated vs. 1.9 x 10^{-2} s^{-1} observed). Also, the observed vorticity maximum occurred at the wave ridge, with the simulated vorticity maximum occurring only 100 s ahead of the wave ridge.

It should be noted that radar volume scans were only available about every 300 s, so *exact* timing and vorticity maxima are subject to some error. Given the available data, even though the timing and magnitude were *somewhat* in error, the overall pattern of a vorticity increase followed by a decrease, associated with passage of a wave trough and ridge, is simulated fairly well even for the first wave ridge. The vorticity change associated with interaction with the second wave ridge
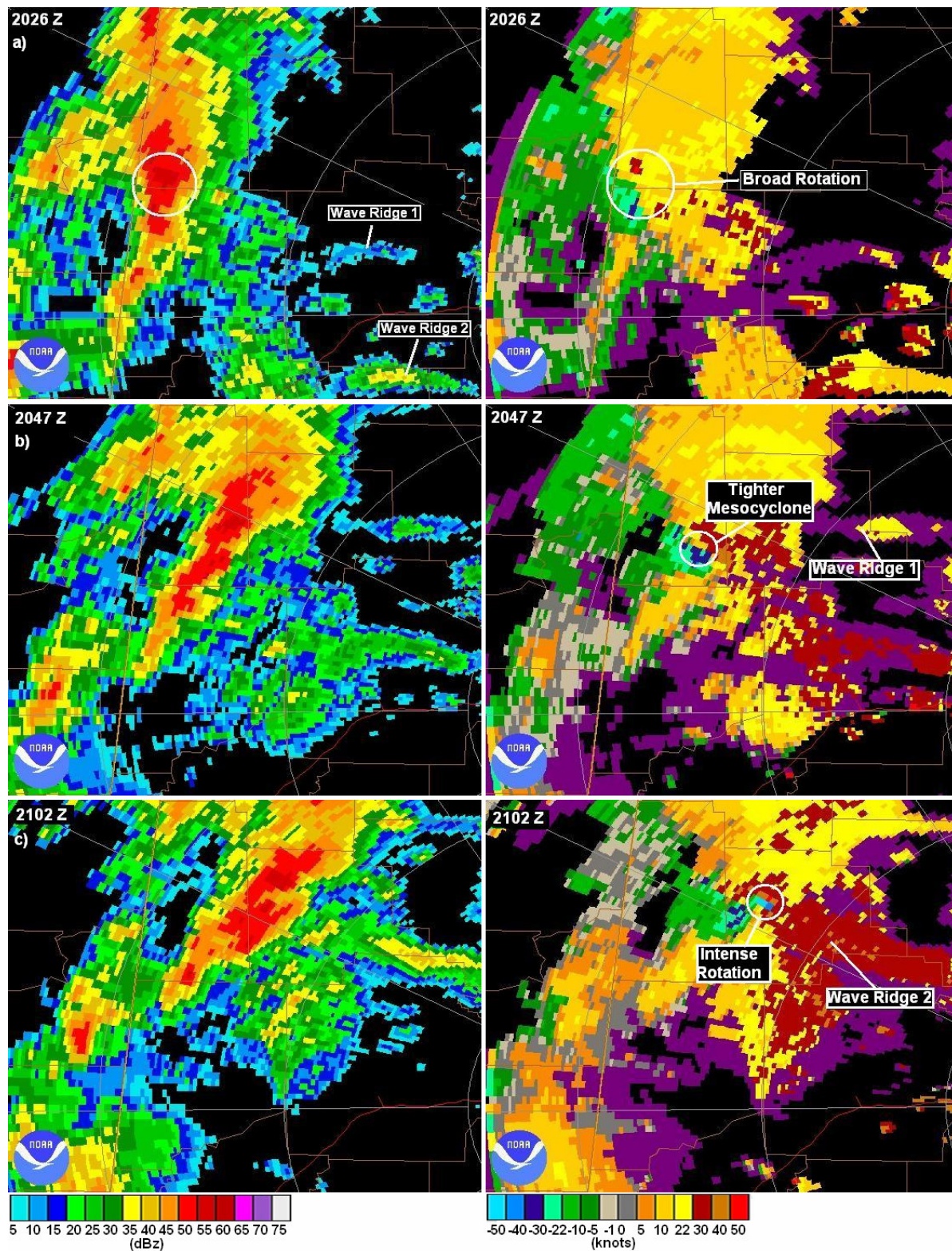
Figure 9. BMX WSR-88D 0.5 degree elevation base reflectivity (left) and storm-relative velocity (right) at a) 2026, b) 2047, and c) 2102 UTC, 22 January 1999 (range rings at 50 km intervals)
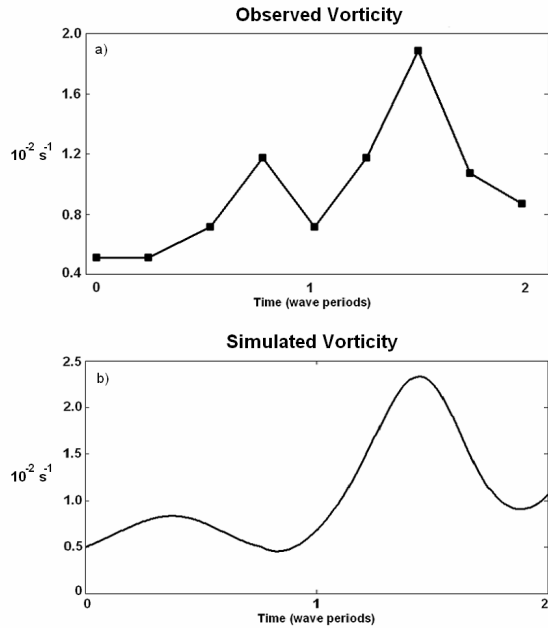
Figure 10. a) Doppler-radar observed mesocyclone vorticity, and b) simulated vorticity for 22 January 1999 case.

is simulated very well, in both time and magnitude. Also, the pattern of a *net increase* in vorticity over a full wavelength, shown in the simulation, is observed.

4) SUMMARY

In summary, an environment favorable for the generation and maintenance of ducted gravity waves existed over western Alabama on the afternoon of 22 January 1999. Fine lines on radar, moving rapidly northward at speeds near 34 m s^{-1}, do indeed represent the ridges of ducted gravity waves. This is based on several facts. 1) The observed speed is consistent with ducted gravity waves in this environment. 2) The fine lines do not represent an undular bore, as the lead fine line is *not* the most intense (neither in its reflectivity presentation nor in its effect on the mesocyclone). 3) The fine lines do not represent density currents. Density currents do not typically move in pairs. Also, based on the equations developed by Seitter (1986), such a speed would require a pressure rise associated with each of the density currents of 8 hPa, ie., a 2 km deep cold pool with a 10 K temperature drop, which is physically unreasonable. The

ducted gravity waves interacted with a pre-existing mesocyclone.

The mesocyclone intensified somewhat upon interaction with the first wave ridge, weakened temporarily between ridges, and intensified further upon interaction with the second wave ridge. These observations are consistent with the theory outlined in section 2b, and with the numerical simulation (section 4a3.)

b) Other Cases
1) 16 DECEMBER 2000

We have identified at least 15 other cases in which, upon preliminary examination of radar data, it appears that a mesocyclone may have intensified and/or been associated with tornadogenesis upon interaction with one or more gravity wave(s). Two of these cases are summarized here to illustrate the common patterns of gravity wave/mesocyclone interaction.

One such case involves the F4 tornado which moved through parts of Tuscaloosa, Alabama, on 16 December 2000, causing 11 fatalities and 144 injuries (*Storm Data*). In this case, despite an unseasonably high CAPE (~900 J kg^{-1}), the nearby 1800 UTC Birmingham, Alabama (BMX) sounding indicated a stable layer, primarily between 1 and 2 km MSL, with N as high as 0.014 s^{-1} at 1600 m MSL. This, combined with very strong wind shear, contributed to a fairly significant ducting layer in the vertical profile of m^2, near 2100 m MSL. In the 1700-2100 m MSL layer, the average value of m^2 was 4.2 x 10^{-6} m^{-2}, while in the 2100-2500 m MSL layer, it was -2.4 x 10^{-6} m^{-2}. Using the ducting theory of Lindzen and Tung (1976), this environment would support ducted gravity waves with speeds of 32 m s^{-1}.

A supercell thunderstorm approached Tuscaloosa from the southwest (about 230 degrees) at 1826 UTC. This storm was part of a weakly-organized convective line, but had already been the strongest storm within at least a 50 km radius since about 1800 UTC, and had shown supercell characteristics since at least 1800 UTC. Meanwhile, at least one fine line in the radar reflectivity field, apparently representing a gravity wave ridge, approached from the SSW (200 degrees) at 32 m s^{-1}, which is also the ducted wave speed calculated

theoretically. When the wave ridge intersected the storm at 1841 UTC, rotational velocity and vorticity increased quickly, and a tornado formed at 1854 UTC (*Storm Data*). The patterns of reflectivity and storm-relative velocity associated with this interaction (Figure 11) are similar to those described in section 4a.
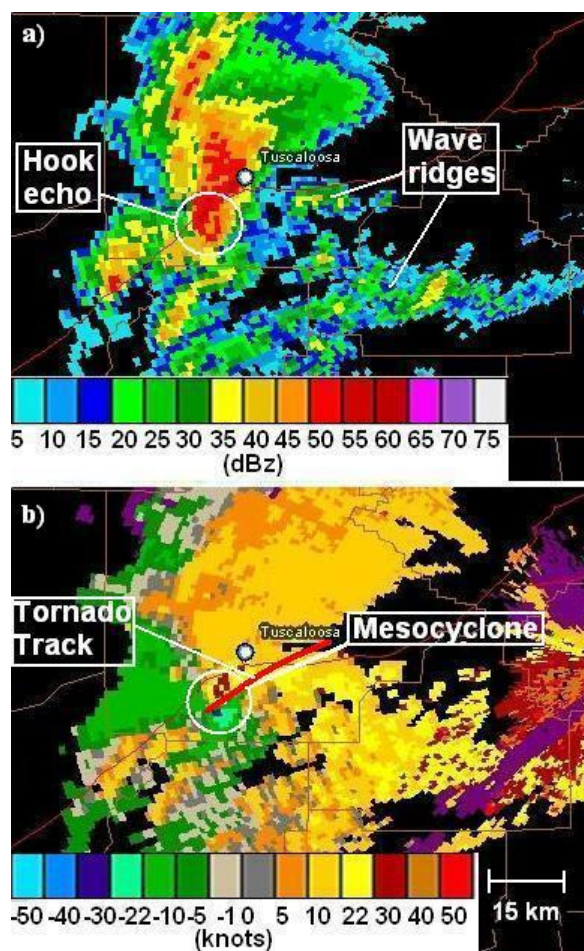

Figure 11. BMX WSR-88D radar imagery at 1857 UTC, 16 December 2000 (at 0.5 degrees elevation). a) reflectivity and b) storm-relative velocity.

2) 8 APRIL 1998

Another case involves the F5 tornado in metropolitan Birmingham, Alabama, on 8 April 1998, which caused 32 fatalities and 258 injuries (*Storm Data*). The tornado examined here was one of a family of tornadoes produced by a classic, long-lived supercell storm. It formed around 09/0042 UTC, and remained on the ground for 46 minutes.

A fine line appeared in radar reflectivity over south-central Alabama as early as 2029 UTC, about 125 km southeast of the eventual path of the tornado. This fine line may have been associated with a density current produced by earlier convection in south Alabama (Pence and Peters 2000). It traveled NNW rather slowly (averaging 6.7 m s^{-1}) between 2030 and 2304 UTC, and then accelerated rather substantially to an average speed of 13.2 m s^{-1} between 2335 UTC and 0032 UTC. The Scorer parameter profile and sounding analysis (from BMX at 18 UTC on 8 April 1998 and 00 UTC on 9 April 1998) based on the theory of Lindzen and Tung (1976) indicate that the speed of the fine line before 2304 UTC is not consistent with ducted gravity waves. In fact, it is more consistent with a density current.

It should be noted that local sunset occurred at 0013 UTC. The 00 UTC sounding, in this case, was released at 2300 UTC, but already indicates some radiative cooling at the surface, producing a shallow stable layer. Surface observations from nearby BHM indicate that temperatures at 2300 UTC had already cooled about 1.7 K below their maximum values for the day, and cooled an additional 0.9 K between 2300 and 0000 UTC. The speed of the fine line during the one-hour period just before it interacted with the supercell (13.2 m s^{-1}) is consistent either with ducted gravity waves of little vertical extent, or, more likely, with a bore, which could have been produced by the density current impinging on the rapidly-evolving stable NBL (e.g., Knupp 2006). If one assumes an inversion 100 m deep, and the bore is about 500 m deep, the bore speed determined using hydraulic theory and the *surface* gravity wave speed for the NBL (e.g., Rottman and Simpson 1989; Simpson 1997, Knupp 2006) would be near 11.2 m s^{-1}, which is very close to the observed speed. The fact that the fine line was accelerating with time is also consistent with a density current-bore transition, as the stable boundary layer would be deepening with time after sunset.

The fascinating aspect of this case lies in the fact that the tornado was already on the ground before interaction with the main reflectivity fine line. However, upon intersection of the wave ridge/bore with the mesocyclone,
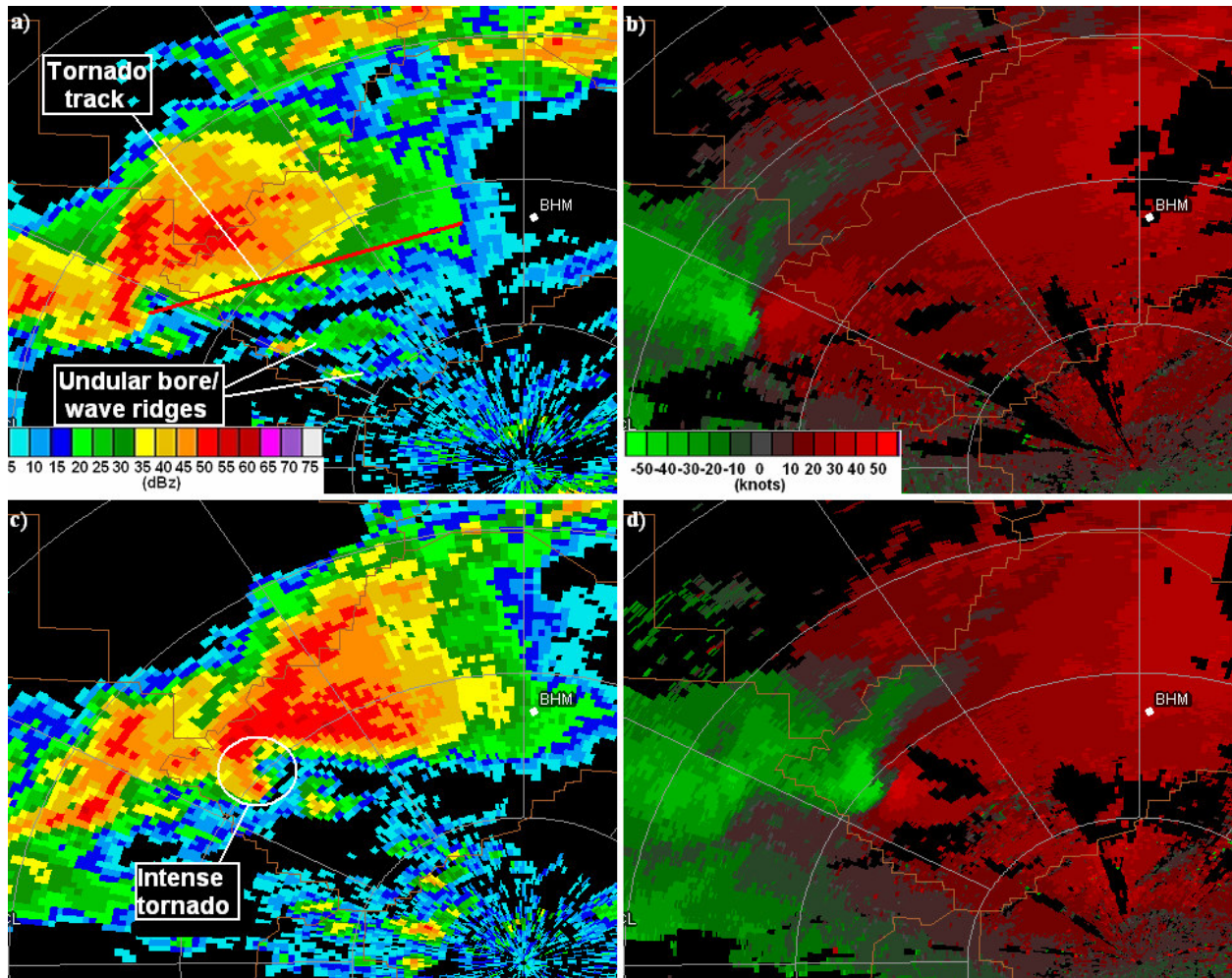
Figure 12. BMX WSR-88D radar imagery from 9 April 1998. a) 0042 UTC reflectivity, b) 0042 UTC base velocity, c) 0058 UTC reflectivity, and d) 0058 UTC base velocity. The tornado initially touched down around 0042 UTC, and the width and damage intensity quickly increased around the time of the intersection of the tornado with the main wave ridge/bore, between 0053 and 0058 UTC (Pence and Peters 2000). All scans are at 0.5 degrees elevation. Range rings are at 25 km intervals.

the tornado damage being produced by the storm rapidly intensified from a narrow-path F0 tornado to a 1 km wide F3 tornado (Pence and Peters 2000). It is possible that, in this case, the wave/bore process enhanced the tornado through the same processes that a wave enhances a mesocyclone, described in section 2b. Radar imagery from the time of tornado touchdown (0042 UTC, before intersection with main reflectivity fine line) and 16 minutes later (0058 UTC, a few minutes after intersection with main fine line) is shown in Figure 12. This interaction, and its result, are similar to that of the previous two cases.

5. Discussion and Conclusions

In this paper, evidence is presented that supports the hypothesis that gravity waves, upon interaction with pre-existing mesocyclones, may significantly alter the vorticity of those mesocyclones, potentially leading to tornadogenesis. This evidence includes theory, numerical simulations, and observations. Such interactions have been speculated upon by previous authors (e.g., Miller and Sanders 1980), and even observed by Kilduff (1999) and Barker (2006). However, this paper examines these interactions in greater detail and provides a dynamical explanation for the observed behavior.

The theoretical airflow within a ducted gravity wave shows significant convergence ahead of the wave ridge and divergence ahead of the wave trough, both of which would enhance/diminish vorticity through the stretching process. Also, with horizontal motion maximized near the surface and vertical motion maximized near the top of the duct (Fig. 2), significant perturbation vertical wind shear is associated with gravity waves. This perturbation shear produces horizontal vorticity, which may be tilted into the vertical by the horizontal gradients in vertical motion associated with a storm updraft, further altering the vorticity of the mesocyclone. The magnitude of this tilting is determined in part by the angle at which the gravity wave intersects the storm inflow vector.

It is clear that a better understanding of ducted gravity wave kinematics is required to quantify this interaction. As a first step, Coleman and Knupp (2008, submitted) show theoretically and in a case study that passage of a ducted gravity wave may drastically change the local storm-relative helicity in a relatively short time (i.e., 60 minutes).

A simple one-dimensional model was developed, considering only the stretching and tilting processes. The model results indicated that the interaction between the gravity wave and the mesocyclone clearly has a significant effect on the vertical vorticity. After a small decrease ahead of the wave trough, ζ increased dramatically (to three times its initial value) just ahead of the wave ridge. The most rapid increase was in the ¼ horizontal wavelength behind the wave trough, where positive perturbation shear produced positive tilting, and convergence generated positive stretching. The vorticity then decreased rapidly behind the wave ridge. However, as noted, *interaction with one wavelength of a gravity wave produced a net increase in mesocyclone vorticity*. This net change was reversed if the wave approached the storm from its left flank, a situation not often observed.

Various numerical simulations showed that maximum mesocyclone vorticity produced by the interaction with a gravity wave increases with larger values of wave amplitude, wavelength, and angle α (over the interval $0 < \alpha < \pi/2$), and decreases with larger wave speed and duct depth. These observations make physical sense. Larger wave amplitude implies larger magnitudes of tilting and stretching, while longer wavelengths (at constant wave speed) mean longer wave periods and more time for stretching and tilting processes to occur. As the angle α between the wave motion vector and the storm inflow vector increases (over the interval $0 < \alpha < \pi/2$), the horizontal vorticity produced by the perturbation shear associated with the wave becomes more streamwise. With larger wave speed (at constant wavelength), wave period decreases, so there is less time for the tilting and stretching processes to occur. Finally, as duct depth increases, so does the vertical wavelength of the gravity waves; so, for constant amplitude, the vertical shear decreases.

The one-dimensional model was used to simulate the 22 January 1999 wave/mesocyclone interaction, with *very good results*. In this case, the mesocyclone interacted with two gravity wave ridges. Observed and simulated peak vorticity values associated with the main wave ridge were similar in magnitude, and occurred with a time error of only 1/12 of a wave period.

Despite the surprisingly good performance of the simple one-dimensional model, a much more robust two-dimensional model is currently under construction. This model will take into account many additional factors including solenoidal vorticity generation, changes in storm-inflow produced by the gravity wave perturbation wind field, and vertical advection of vorticity. This model, once

completed, will be used to validate and refine the results of the one-dimensional model, and will be used to simulate other cases of wave/mesocyclone interaction.

In the 22 January 1999, 16 December 2000, and 8 April 1998 cases, vorticity changes were observed using Doppler radar data, and were consistent with those predicted by theory. The 22 January 1999 case proved to be very useful in that two gravity wave ridges interacted with the mesocyclone, producing a periodic increase and decrease in mesocyclone vorticity, with an overall increase after interaction with two wave ridges. In the 16 December 2000 case, mesocyclone vorticity increased as the wave ridge(s) approached, and tornadogenesis occurred around the time of intersection with the first wave ridge. The 8 April 1998 case presents a unique challenge, as it appears that the waves interacting with the storm were part of an undular bore. Also, in this case, the tornado was already occurring prior to the intersection with the main fine line/wave ridge, but the tornado intensified dramatically around the time the intersection occurred. In general, observations and initial model results support the hypothesis that gravity waves significantly alter the vorticity of mesocyclones with which they interact, sometimes resulting in tornadogenesis.

In addition to analysis of other case studies and improved, two-dimensional numerical simulations, the physics of the interaction between gravity waves and mesocyclones can be better understood with more precise measurements of gravity wave kinematics and details of the mesocyclone response, using multiple-Doppler radar syntheses. It is hoped that such an interaction will occur during VORTEX2 in 2009 and 2010, allowing for a detailed analysis. Finally, more targeted measurements of the convergence and shear profiles within ducted gravity waves, using the UAH mobile measurement platforms (MIPS, Karan and Knupp 2006), the Mobile Alabama X-band dual polarization radar (MAX), and the fixed-site Advanced Radar for Meteorological and Operational Research (ARMOR, Petersen et al. 2007) will allow for even better modeling of the interaction process.

References

Alexander, M. J., J. R. Holton, and D. R. Durran, 1995: The gravity wave response above deep convection in a squall line simulation. *J. Atmos. Sci.*, **52**, 2212-2226.

Barker, L. J., 2006: A potentially valuable WSR-88D severe storm pre-cursor signature in highly dynamic, low CAPE, high shear environments. Extended abstracts, *23rd Conf. on Severe Local Storms*, American Meteorological Society.

Bosart, L. F., and J. P. Cussen, 1973: Gravity wave phenomena accompanying East Coast cyclogenesis. *Mon. Wea. Rev.*, **101**, 446-454.

Coleman, T. A., and K. R. Knupp, 2008: Rapid local changes in storm-relative helicity associated with a ducted gravity wave. *Mon. Wea. Rev.*, submitted.

Corfidi, S. F., 1998: Some thoughts on the role mesoscale features played in the 27 May 1997 central Texas tornado outbreak. Preprints, *19th Conf. on Severe Local Storms*, American Meteorological Society.

Cram, J. M., R. A. Pielke, and W. R. Cotton, 1992: Numerical simulation and analysis of a prefrontal squall line. Part II: Propagation of the squall line as an internal gravity wave. *J. Atmos. Sci.*, **49**, 209-225.

Davies-Jones, R., 1984: Streamwise vorticity: The origin of updraft rotation in supercell storms. *J. Atmos. Sci.*, **41**, 2991-3006.

Droegemeier, K. K., S. M. Lazarus, and R. Davies-Jones, 1993: The influence of helicity on numerically simulated convective storms. *Mon. Wea. Rev.*, **121**, 2005-2029.

Karan, H., and K. Knupp, 2006: Mobile Integrated Profiler System (MIPS) observations of low-level convergent boundaries during IHOP. *Mon. Wea. Rev.*, **134**, 92-112.

Kilduff, R. E., 2006: Personal communication.

Kilduff, R. E., 1999: The interaction of a gravity wave with a thunderstorm. Electronic poster, NOAA/National Weather Service.

Knupp, K. R. (2006): Observational analysis of a gust front to bore to solitary wave transition within an evolving nocturnal boundary layer. *J. Atmos. Sci.*, **63**, 2016-2035.

Koch, S. E., D. Hamilton, D. Kramer, and A. Langmaid, 1998: Mesoscale dynamics in the Palm Sunday tornado outbreak. *Mon. Wea. Rev.*, **126**, 2031-2060.

Koch, S. E., and C. O'handley, 1997: Operational forecasting and detection of mesoscale gravity waves. *Wea. Forecasting*, **12**, 253-281.

Koch, S. E., R. E. Golus, and P. B. Dorian, 1988: A mesoscale gravity wave event observed during CCOPE. Part II: Interactions between mesoscale convective systems and the antecedent waves. *Mon. Wea. Rev.*, **116**, 2545-2569.

Lalas, D. P., and F. Einaudi, 1976: On the characteristics of gravity waves generated by atmospheric shear layers. *J. Atmos. Sci.*, **33**, 1248-1259.

Lindzen, R. S., and K. –K. Tung, 1976: Banded convective activity and ducted gravity waves. *Mon. Wea. Rev.*, **104**, 1602-1617.

Miller, D. A., and F. Sanders, 1980: Mesoscale conditions for the severe convection of 3 April 1974 in the East-Central United States. *J. Atmos. Sci.,* **37,** 1041-1055.

Pence, K. J., and B. E. Peters, 2000: The tornadic supercell of 8 April 1998 across Alabama and Georgia. Preprints, *20th Conf. on Severe Local Storms,* Amer. Meteor. Soc.

Petersen, W.A., K. R. Knupp, D. J. Cecil, and J. R. Mecikalski, 2007: The University of Alabama Huntsville THOR Center Instrumentation: Research and operational collaboration. 33rd Conference on Radar Meteorology, 6-10 August 2007, Amer. Meteor. Soc.

Raymond, D. J., 1984: A wave-CISK model of squall lines. *J. Atmos. Sci.*, **41**, 1946-1958.

Rottman, J. W., and Simpson J. E., 1989: The formation of internal bores in the atmosphere: A laboratory model. *Quart. J. Roy. Meteor. Soc.,* **115**, 941–963.

Scorer, R., 1949: Theory of waves in the lee of mountains. *Quart. J. Roy. Meteor. Soc.,* **75,** 41–56.

Seitter, K. L., 1986: A numerical study of atmospheric density current motion including the effects of condensation. *J. Atmos. Sci.,* **43**, 3068-3076.

Simpson, J. E., 1997: *Gravity Currents: In the Environment and the Laboratory.* 2d ed. Cambridge University Press, 244 pp.

Stobie, J. G., F. Einaudi, and L. W. Uccellini, 1983: A case study of gravity waves-convective storms interaction: 9 May 1979. *J. Atmos. Sci.*, **40**, 2804-2830.

Uccellini, L. W., and S. E. Koch, 1987: The synoptic setting and possible energy sources for mesoscale wave disturbances. *Mon. Wea. Rev.*, **115**, 721-729.

Uccellini, L. W., 1975: A case study of apparent gravity wave initiation of severe convective storms. *Mon. Wea. Rev.*, **103**, 497-513.